Computational Methods for Differential Equations
http://cmde.tabrizu.ac.ir
Vol. 9, No. 1, 2021, pp. 273-288
DOI:10.22034/cmde.2020.35593.1611

Application of the method of fundamental solutions for designing the optimal shape in heat transfer

Kamal Rashedi*
Department of Mathematics,
University of Science and Technology of Mazandaran, Behshahr, Iran.
E-mail: k.rashedi@mazust.ac.ir

Akbar Hashemi Borzabadi
Department of Mathematics,
University of Science and Technology of Mazandaran, Behshahr, Iran.
E-mail: borzabadi@mazust.ac.ir

Maryam Zarhoun
Department of Mathematics,
University of Science and Technology of Mazandaran, Behshahr, Iran.
E-mail: mzflower91@yahoo.com

Abstract In this paper, we propose a meshless regularization technique for solving an optimal shape design problem (OSD) which consists of constructing the optimal configuration of a conducting body subject to given boundary conditions to minimize a certain objective function. This problem also can be seen as the problem of building a support for a membrane such that its deflection is as close as possible to 1 in the subset D of the domain. We propose a numerical technique based on the combination of the method of fundamental solutions and application of the Tikhonov's regularization method to obtain stable solution. Numerical experiments while solving several test examples are included to show the applicability of the proposed method for obtaining the satisfactory results.

Keywords. Elliptic equation, Optimal shape, Method of fundamental solutions, Tikhonov regularization, Radial basis functions.

2010 Mathematics Subject Classification. 35A08, 65N80, 35R35, 49K20, 34H05.

1. Introduction

Mathematical models describing the thermal processes for determination of the optimal shape of a heat conducting body with respect to a specified design criterion, belong to the category of inverse heat transfer problems (IHTPs). Historically, the inverse heat transfer problems were first appered in early 1960's to support the space programs where it was impossible to figure out the temperature at the surface of the thermal shields of space vehicles [18]. On the other hand, it was much easier to derive information by placing some sensors at the interior parts with a specified distance from the surface. Therefore, by employing an inverse analysis of the information

Received: 13 September 2019 ; Accepted: 12 January 2020.
$*$ corresponding.

exploited from the sensors, the temperature at the surface was approximated [18, 19]. Generally speaking, in the theory of heat transfer problems, if boundary conditions, the thermophysical properties or the geometrical configuration of the heated body are uknown then the problem is referred to as inverse heat transfer problem. Todays, traces of inverse heat transfer problems can be found in different areas of science and engineering because of their great mathematical applications [14, 15]. To name a few applications, we can refer to [18, 19, 20] the electronic packaging problems where designing an appropriate shape for the electronic devices prevents damage. Moreover, in the chemical vapor deposition (CVD) process, producing the fine solid materials depends on providing uniform temperature distribution in the deposition zone across the surface of the substrate.

The steady-state heat transfer problems may consist of finding the optimal shape of a body such that either the temperature distribution on its boundary or the heat flux on some part of its boundary match a desired distribution. Optimal shape design problems (OSD) model many applied problems of science and industry such as finding the optimal structures of a car such that the final production carries the minimum weight while having the best aerodynamics, designing the best breakwater to protect a harbor from uniformly sinusoidal waves with a determined wave length and direction and optimization of stealth objects and antenna subject to aerodynamic constraints in electromagnetism [17]. Mathematically speaking, the OSD problems deal with solving an optimization problem where the dynamic constrains are a system of partial differential equations defined over a physical domain Ω supplemented with boundary conditions.

Following, we consider an OSD problem which has great applications in wind tunnel or nozzle design for potential flows [17]. For this problem, some of the boundary conditions are defined over an unknown curve $\Gamma^* \subset \partial\Omega$. We address the question of simultaneous estimation of the unspecified trajectory function Γ^* as well as the stream function by applying the given boundary conditions and using the fact that the volume of the stream function passing through the known region $D \subset \Omega$ reaches a prescribed value.

1.1. **Problem statement and some applications:** Assume that an incompressible irrotational flow at each location $(x, y) \in \Omega \subset \mathbb{R}^2$, denoted by stream function $\psi(x, y)$, satisfies the Poisson equation

$$\triangle\psi = g \quad in \quad \Omega, \tag{1.1}$$

such that (see Figure 1)

$$\partial\Omega = \Gamma_1 \cup \Gamma_2 \cup \Gamma_3 \cup \Gamma^*, \quad \Gamma_1 = \{0\} \times [0, a],\ \Gamma_2 = \{L\} \times [0, b],\ \Gamma_3 = [0, L] \times \{0\},$$

$$\Gamma^* := \{(x, s(x))|\ s \in C[0, L],\ s(0) = a,\ s(L) = b\}. \tag{1.2}$$

The mathematical representation of the shape optimization problem of interest here is expressed by [17]:

$$\mathbf{P} := \min_{\partial\Omega,\ D\subset\Omega} \left\{ \int_D (\psi - 1)^2 \quad s.t \quad \Delta\psi = g, \quad \psi|_{\partial\Omega} = 0 \right\}, \tag{1.3}$$

FIGURE 1. Representation of the physical domain corresponding to problem **P**, with locations of the given bounderies $\Gamma_1,\ \Gamma_2,\ \Gamma_3$ and unknown moving boundery Γ^*.

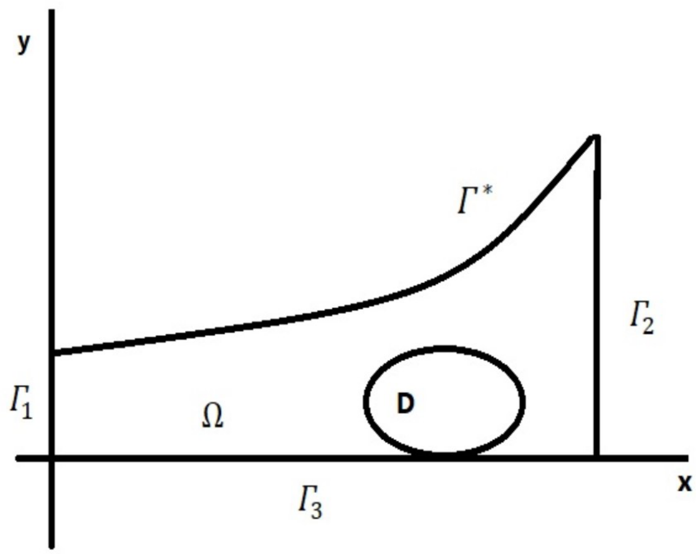

FIGURE 2. Representation of a possible placement of source ($\circ$) and collocation points ($\star$).

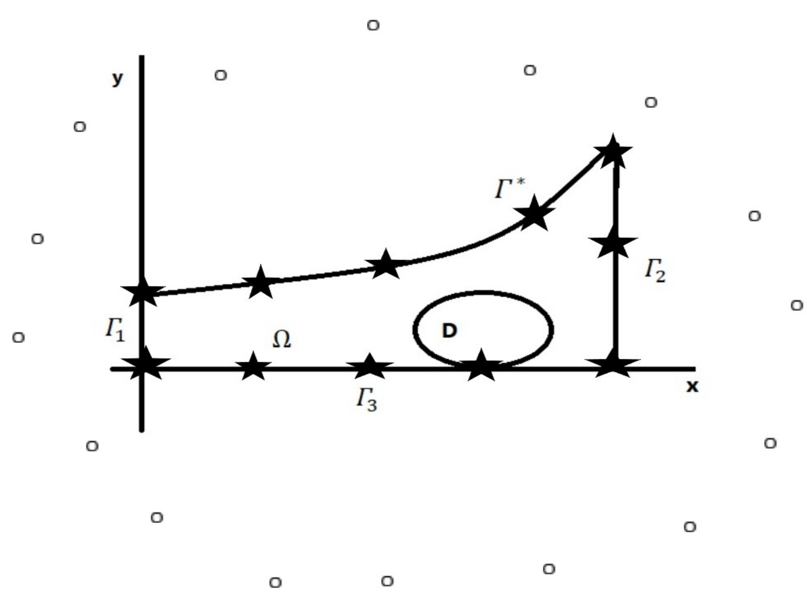

where the notation $\psi|_{\partial\Omega} = 0$ stands for the Dirichlet boundary conditions on $\partial\Omega$ as follows:

$$\psi(0, y) = 0,\ 0 < y < a, \quad \psi(L, y) = 0,\ 0 < y < b,$$
$$\psi(x, 0) = \psi(x, s(x)) = 0, \quad 0 < x < L.$$

In general, g is a multivariate function but when g is a constant function, more specially, when $g(x, y) = 9.81$, we pose the following question: Is it possible to build a support for a membrane with domain Ω bent by its own weight which would bring its deflection as close to 1 as possible in a region of space $D \subset \Omega$?

A rigorous proof of the shape design sensitivity formulas for the static response and the repeated eigenvalues of the membrane has been discussed in [32]. Since the solution is sensitive to errors with respect to boundary conditions, we use the Tikhonov regularization method to achieve stable numerical solution.

1.2. **Literature review:** As a special case of 2D optimal control problems [7, 16], various methods have been applied to solve OSD problems. These studies include classical approaches such as dynamic interpretation of OSD, applying some direct calculations of shape variations, employing the minimax differentiability method and using the mapping method [2, 4, 5, 9, 10, 11]. Moreover, finite element methods and measure theoretical techniques have also been employed in the literature [1, 21, 22, 24, 25]. Other numerical approaches such as evolutionary algorithms including the genetic algorithm, topological optimization and level set algorithms, iterative optimization techniques such as Newton, quasi Newton and conjugate gradient have been discussed in [17, 18, 19, 24, 25] and references therein.

In this work, since the optimization problem involves partial differential equation with its constrains, we aim to employ the method of fundamental solutions (MFS), which is a meshless boundary collocation technique and belongs to the class of Trefftz method [12, 13, 35]. We solve the Poisson equation defined over a domain Ω by approximating the stream function ψ using the method of fundamental solutions. The following is a list of key points that jutifies why the method of fundamental solutions is suitable for solving the considered problems:

- The MFS is easy to adjust to various solution domains by applying a scattered set of points on the irregular domains [8] like Ω. In contrast other approximations based on the use of finite-difference methods (FDM), finite element methods (FEM) and orthogonal polynomials have shortcomings in dealing with problems defined over nonrectangular domains, especially in higher dimensions [26, 29, 31].
- The MFS is easy to program and it is computationally cost-effective. On contrast, the mesh dependent methods, such as classical and modified spectral element methods (SEM) and finite element methods (FEM) suffer from a large computational time, while in MFS no mesh generation is needed because it employs the collocation technique [30, 31].

- Despite the fact that MFS results in ill-conditioned matrices, the usage of regularization techniques leads to accurate and stable results for different types of problems [31].
- The literature on application of method of fundamental solutions for the homogenous partial differential equations is rather extensive, but in this work we deal with the nonhomogenous case (Poisson equation). This motivates us to develop the application of the method of fundamental solutions in recovering the stream function ψ using the dual reciprocity method [6, 23, 27].

1.3. **The structure of this paper:** This paper is organized as follows. In section 2, we propose a numerical algorithm for solving the given inverse problem based on the method of fundamental solutions. In section 3, we present the numerical results. In section 4, we give some concluding remarks on the results of the paper.

2. The solution procedure

It should be noted that for applying the method of fundamental solutions, a general placement of source and collocation points similar to Figure 2 is required. Then, we take into account the fundamental solution [12] of the two dimensional Laplace equation as:

$$\Phi(x,y) = \log(x^2+y^2), \qquad (x,y) \in \Omega. \tag{2.1}$$

The source points should be located outside the domain. We are interested in setting the source points, placed external to the domain Ω via the following construction scheme:

$$\Gamma_P := \left\{ (x_j^0, y_j^0) |\ x_j^0 = \frac{L}{2} + (\frac{L}{2}+\gamma)\cos\left(\frac{2\pi j}{N_1}\right),\ y_j^0 = \frac{b}{2} + (\frac{b}{2}+\gamma)\sin\left(\frac{2\pi j}{N_1}\right),\ j = \overline{1, N_1} \right\}, \tag{2.2}$$

where $\gamma > 0$ and use a linear combination of basis functions belong to the following set

$$\left\{ \Phi_m(x,y) = \Phi(x - x_m^0, y - y_m^0) \right\}_{m=1}^{N_1}. \tag{2.3}$$

To solve the problem **P** where the function g is a two dimensional function, say $g := g(x,y)$, we use (2.2) for placing the source points and consider the following approximation for ψ:

$$\overline{\psi(x,y)} = \sum_{m=1}^{N_1} c_m \Phi_m(x,y) + \psi_p(x,y), \tag{2.4}$$

where $\psi_p(x,y)$ is supposed to satisfy the following equation:

$$\Delta\left\{ \psi_p(x,y) \right\} = g(x,y). \tag{2.5}$$

Also, we introduce a Ritz type approximation [28, 33] using a truncated series in terms of the Lagrange polynomials $L_i(x)$ [26]:

$$\overline{s(x)} = \sum_{m=N_1+1}^{N_1+N_2} c_m x(x-L)L_i(x) + a + \frac{(b-a)x}{L}, \quad 0 \le x \le L, \tag{2.6}$$

as an approximation for the smooth object $s(x)$, where c_i's are the unknown coefficients. Moreover, it is obvious that the conditions $s(0) = a,\ s(L) = b$ are satisfied. Next, we apply the dual reciprocity technique to calculate $\psi_p(x, y)$. The main idea consists of four steps:

Step1: Use the radial basis functions [3, 29] to approximate the known function $g(x, y)$. For which, we assume that this approximation is derived by using the IMQ radial basis function $F(x, y) = \frac{1}{\sqrt{x^2+y^2+\epsilon^2}}, \quad \epsilon \in \mathbb{R}$.

Step2: Apply the collocation points (x_k, y_k) belonging to the domain Ω and solve the interpolation problem

$$g(x_k, y_k) - \sum_{j=1}^{M} d_j F(x_k - x_j, y_k - y_j) = 0, \quad k = \overline{1, M}, \tag{2.7}$$

then find the elements $d_i,\ i = \overline{1, M}$.

Step3: Apply the annihilator method [6, 27] to get $Z(r)$ by solving the following differential equation:

$$\frac{1}{r}\frac{d\left(r\frac{dZ(r)}{dr}\right)}{dr} = \frac{1}{\sqrt{r^2+\epsilon^2}}, \quad r = \sqrt{x^2+y^2} \tag{2.8}$$

and get

$$Z(r) = \sqrt{r^2+\epsilon^2} + \epsilon\log(\epsilon^3 r) - \epsilon\log\left(2\epsilon^2 + 2\epsilon\sqrt{r^2+\epsilon^2}\right) + A\log(r) + B, \quad A, B \in \mathbb{R}. \tag{2.9}$$

Step4: Establish the approximation $\psi_p(x, y) = \sum_{j=1}^{M} d_j Z(x-x_j, y-y_j),\ (x_j, y_j) \in \Omega$.

To fulfill the following Dirichlet boundary conditions

$$\psi(0, y) = 0,\ y \in [0, a], \qquad \psi(L, y) = 0,\ y \in [0, b], \tag{2.10}$$

$$\psi(x, 0) = 0,\ x \in [0, L], \qquad \psi(x, s(x)) = 0,\ x \in [0, L], \tag{2.11}$$

we construct the new Tikhonov's functional as:

$$\begin{aligned} J^* &= \sum_{i=1}^{M_1}\left\{\sum_{m=1}^{N_1} c_m\Phi_m(0,t_i)+\psi_p(0,t_i)\right\}^2 \\ &+\sum_{i=1}^{M_2}\left\{\sum_{m=1}^{N_1} c_m\Phi_m(L,y_i)+\psi_p(L,y_i)\right\}^2 \\ &+\sum_{i=1}^{M_3}\left\{\sum_{m=1}^{N_1} c_m\Phi_m(x_i,0)+\psi_p(x_i,0)\right\}^2+\lambda\sum_{i=1}^{N_1+N_2} c_i^2 \\ &+\int_D(\sum_{m=1}^{N_1}\Phi_m(x,y)+\psi_p(x,y)-1)^2 \\ &+\sum_{i=1}^{M_3}\left\{\sum_{m=1}^{N_1} c_m\Phi_m(x_i,\overline{s(x_i)})+\psi_p(x_i,\overline{s(x_i)})\right\}^2, \end{aligned} \tag{2.12}$$

and minimize it to get the parameters $c_i,\ i=\overline{1,N_1+N_2}$.

For minimizing J^*, we can either use the necessary conditions for the extremum as

$$\frac{\partial J^*}{\partial c_j}=0, \quad j=\overline{1,N_1+N_2}, \tag{2.13}$$

and solve a nonlinear system of algebraic equations for the elements c_i directly, or apply the Mathematica toolbox "NMinimize" which is designed to minimize a sum of squares of arbitrary differentiable functions. The regularization parameter λ is applied to the functional J^* as a known value. Then, this approach is called as the static MFS. It is worth mentioning that the integration term $\int_D(\sum_{m=1}^{N_1}\Phi_m(x,y)+\psi_p(x,y)-1)^2$ in J^* will be calculated numerically using the midpoint rule [34].

Remark 2.1. It should be noted that **Step2** involves solving an interpolation problem based on the radial basis functions which raises the cost of computations. When the function g is a single variable function, i.e. $g:=g(y)$ we can avoid employing the dual recipricity technique and just use some tranformations to reduce the problem $\Delta\psi=g(y)$ to a homogeneous one and then use the method of fundamental solutuions to solve the new problem. In what follows, we briefly explain the procedure.

First take the transformations

$$U=\psi-G(y), \quad G(y)=\int_0^y\int_0^t g(s)dsdt, \tag{2.14}$$

to get the new modified minimization problem

$$\min_{\partial\Omega,\ D\subset\Omega}\left\{\int_D(U+G-1)^2 \quad s.t \quad \Delta U=0, \quad U|_{\partial\Omega}=\eta\right\}, \tag{2.15}$$

where η stands for the following Dirichlet boundary conditions:

$$U(0,y)=-G(y),\ y\in[0,a], \qquad U(L,y)=-G(y),\ y\in[0,b], \tag{2.16}$$

$$U(x,0)=0,\ x\in[0,L],\qquad U(x,s(x))=-G(s(x)),\ x\in[0,L]. \tag{2.17}$$

Hereafter the solution procedure is straightforward. The approximation for $s(x)$ is assumed exactly like (2.6) and we consider

$$\overline{U(x,y)}=\sum_{m=1}^{N_1} c_m\Phi_m(x,y). \tag{2.18}$$

Then, by minmizing the following Tikhonov's functional

$$\begin{aligned}J_1^*=&\sum_{i=1}^{M_1}\Big\{\sum_{m=1}^{N_1} c_m\Phi_m(0,t_i)+G(t_i)\Big\}^2+\sum_{i=1}^{M_2}\Big\{\sum_{m=1}^{N_1} c_m\Phi_m(L,y_i)+G(y_i)\Big\}^2\\&+\sum_{i=1}^{M_3}\Big\{\sum_{m=1}^{N_1} c_m\Phi_m(x_i,0)\Big\}^2+\lambda\sum_{i=1}^{N_1}c_i^2+\int_D(\sum_{i=1}^{N_1}\Phi_m(x,y)+G(y)-1)^2\\&+\sum_{i=1}^{M_3}\Big\{\sum_{m=1}^{N_1} c_m\Phi_m(x_i,\overline{s(x_i)})+G(x_i,\overline{s(x_i)})\Big\}^2,\end{aligned} \tag{2.19}$$

we get the unknown parameters $c_i,\ i=\overline{1,N_1+N_2}$. It must be noted that the numerical solution obtained by minimizing the functional 2.12 or 2.19 is acceptable as long as $\forall\ x\in[0,L],\ a\le\overline{s(x)}\le b$.

3. Numerical experiments

To test the effectiveness of the proposed technique, we solve two benchmark test examples. They are chosen to report the results of implementing the proposed method. The numerical experiments are carried out in the presence of the maximum tolerable amount of noise level $\lambda\%=\lambda\times10^{-2}$. The numerical implementation is carried out in MATHEMATICA 11, with hardware configuration: Desktop 32-bit Intel Core 7 Duo CPU, 4 GB of RAM, 32-bit Operating System (Windows 10).

Example 3.1. Consider **P** with the following properties:

$$g(x,y)=9.81,\ L=b=3,\ a=1,\ D=[1.5,2.5]\times[0,1]. \tag{3.1}$$

By employing (2.14)-(2.19) with

$$N_1=36,\ N_2=2,\ M_1=M_2=M_3=M_4=4000,\ \gamma=0.2,\ G(y)=\frac{9.81y^2}{2},\ \lambda=10^{-5},$$

we find the results illustrated by Figures 3-4 where the minimum value of the cost functional $\int_D(\psi-1)^2$ is 5.89501. Moreover, by defining

$$\begin{aligned}&U_1(y)=U(0,y)+G(y),\ U_2(y)=U(L,y)+G(y),\\&U_3(x)=U(x,0),\ U_4(x)=U(x,s(x))+G(s(x)),\\&\varepsilon^*=\|U_1(y)\|_2+\|U_2(y)\|_2+\|U_3(x)\|_2+\|U_4(x)\|_2,\end{aligned}$$

FIGURE 3. Approximate solution for $s(x)$ with $\lambda = 10^{-5}$ in presence of exact boundary data, discussed in Example 3.1.

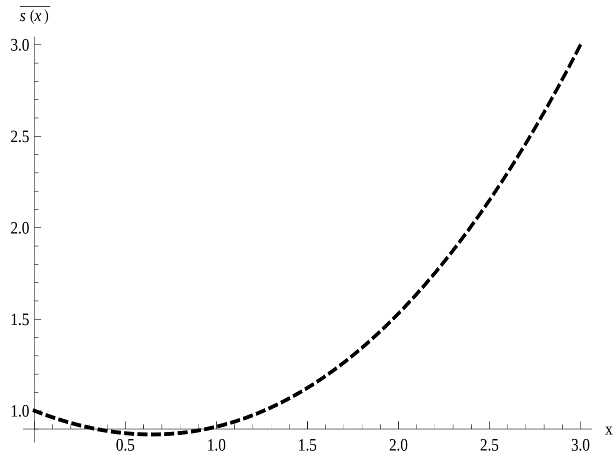

FIGURE 4. Approximate solution for $\psi(x, y)$ with $\lambda = 10^{-5}$ in presence of exact boundary data, discussed in Example 3.1.

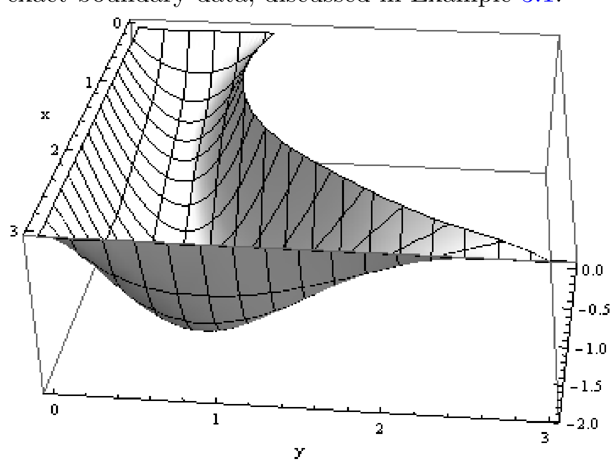

as the residual of the boundary conditions, the obtained results are visualized by Figures 5-8 confirming that the boundary conditions are fulfilled accurately. Next, we

test the numerical stability of the solution by employing the contaminated input boundary data generated by:

$$\psi(0, y_l) = \delta\% RandomReal[\{-1, 1\}], \quad y_l \in (0, 1), \; l = \overline{1, M_1},$$

$$\psi(3, y_l) = \delta\% RandomReal[\{-1, 1\}], \quad y_l \in (0, 3), \; l = \overline{1, M_2},$$

Figure 5. Graph of the absolute error for the residual of boundary condition $U_1(y)$ with $\lambda = 10^{-5}$, $\varepsilon^* = 0.0426153$ in presence of exact boundary data discussed in Example 3.1.

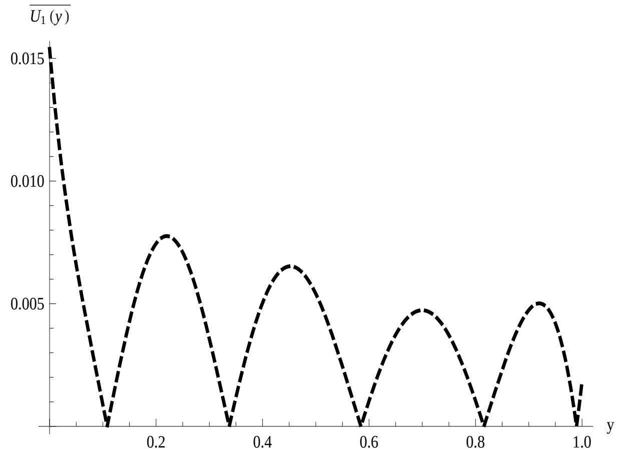

Figure 6. Graph of the absolute error for the residual of boundary condition $U_2(y)$ with $\lambda = 10^{-5}$, $\varepsilon^* = 0.0426153$ in presence of exact boundary data discussed in Example 3.1.

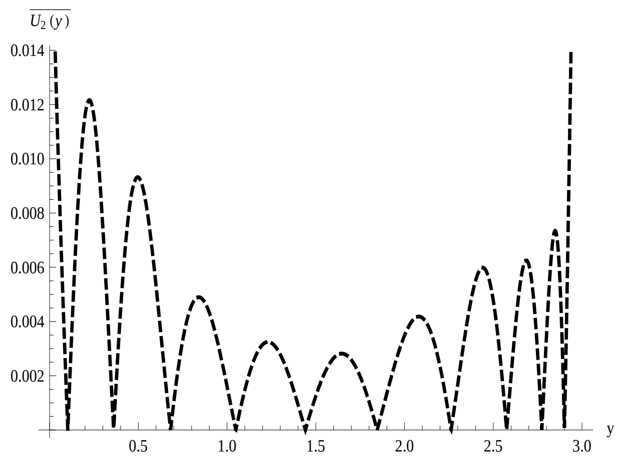

$$\psi(x_l, 0) = \delta\% RandomReal[\{-1, 1\}], \quad x_l \in (0, 3), \ l = \overline{1, M_3},$$

$$\psi(x_l, s(x_l)) = \delta\% RandomReal[\{-1, 1\}], \quad x_l \in (0, 3), \ l = \overline{1, M_4},$$

where $RandomReal[\{-1, 1\}]$ produces a random real digit that belongs to the interval $[-1, 1]$ and $\delta\% = \delta \times 10^{-2}$ is called the level of noises. The results for this experiment are shown in Table 1 to see a good agreement between the exact and approximate

FIGURE 7. Graph of the absolute error for the residual of boundary condition $U_3(x)$ with $\lambda = 10^{-5}$, $\varepsilon^* = 0.0426153$ in presence of exact boundary data discussed in Example 3.1.

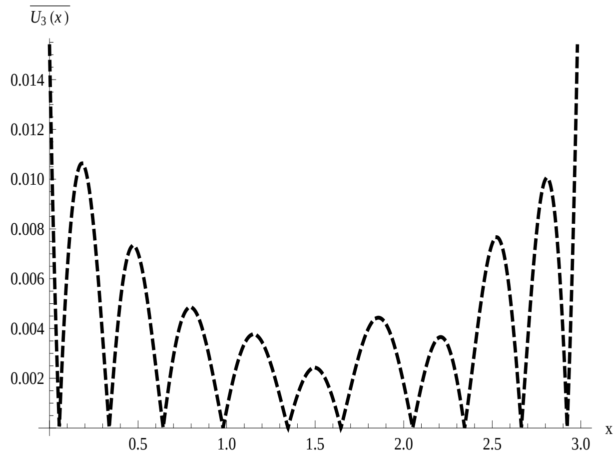

FIGURE 8. Graph of the absolute error for the residual of boundary condition $U_4(x)$ with $\lambda = 10^{-5}$, $\varepsilon^* = 0.0426153$ in presence of exact boundary data discussed in Example 3.1.

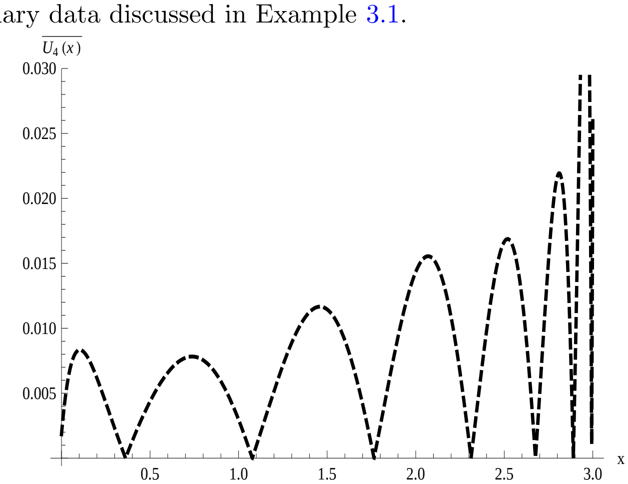

solutions. Nevertheless, when noise level δ increases, according to parameter ε^* the approximations for the boundary conditions depart from the exact solution.

Example 3.2. In this example we discuss solving **P** where

$$g(x, y) = \exp(-x^2 - y^2), \; L = b = 3, \; a = 1,$$

TABLE 1. The obtained values for the cost functional $\int_D(\psi-1)^2$ and ε^* in the present of the different noise levels δ with $N_1 = 36,\ N_2 = 2,\ M_1 = M_2 = M_3 = M_4 = 1000,\ \gamma = 0.2,\ \lambda = 10^{-5}$, discussed in Example 3.1 for exact and contaminated data.

$\delta\%$	0%	1%	3%	7%	10%
ε^*	0.05880	0.08298	0.1625	0.3523	0.4761
$\int_D(\psi-1)^2$	5.5834	5.4224	5.4210	5.2707	5.1700

FIGURE 9. Approximate solution for $s(x)$ with $\lambda = 10^{-7}$ in presence of exact boundary data, discussed in Example 3.2.

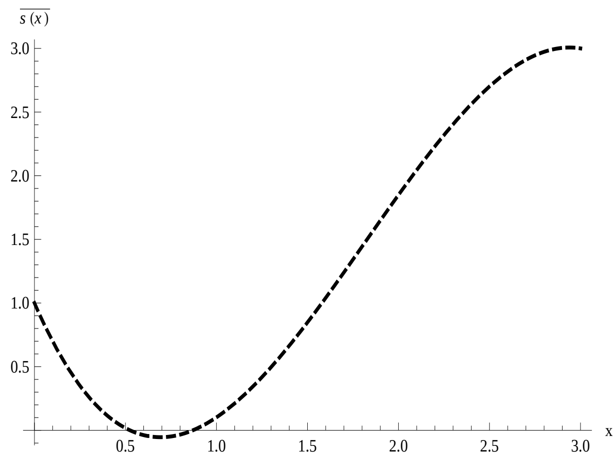

and D is a closed region with boundaries $y = 0,\ y = x-2,\ y = \sqrt{\frac{\pi^2}{16} - (x-2)^2}$. We use the procedure presented by (2.4)-(2.13) with the following parameters

$$N_1 = 46,\ N_2 = 2,\ M_1 = M_2 = M_3 = M_4 = 200,$$
$$M = 100,\ A = B = 0,\ \epsilon = 0.25,\ \gamma = 0.2,\ \lambda = 10^{-7},$$

and obtain the resultes shown by Figures 9-14.

The optimal value of cost function is obtained 0.242832.

FIGURE 10. Approximate solution for $\psi(x, y)$ with $\lambda = 10^{-7}$ in presence of exact boundary data, discussed in Example 3.2.

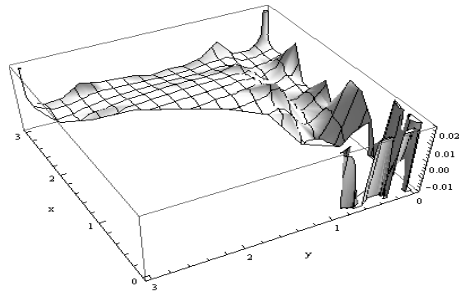

FIGURE 11. Graph of the absolute error for the residual of boundary condition $\psi(0, y)$ with $\lambda = 10^{-7}$ in presence of exact boundary data discussed in Example 3.2.

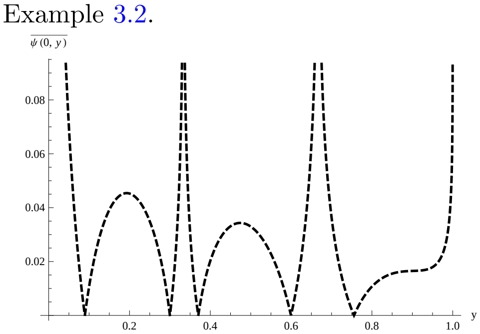

FIGURE 12. Graph of the absolute error for the residual of boundary condition $\psi(3, y)$ with $\lambda = 10^{-7}$ in presence of exact boundary data discussed in Example 3.2.

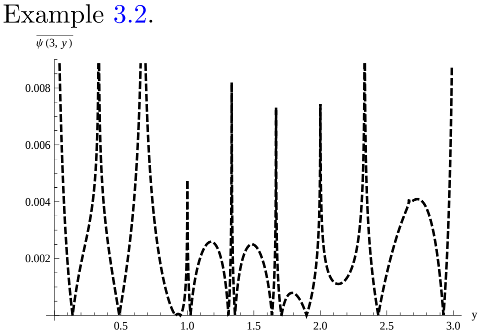

FIGURE 13. Graph of the absolute error for the residual of boundary condition $\psi(x, 0)$ with $\lambda = 10^{-7}$ in presence of exact boundary data discussed in Example 3.2.

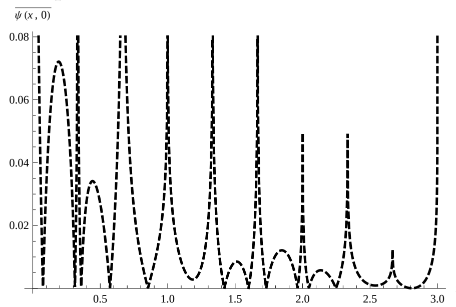

FIGURE 14. Graph of the absolute error for the residual of boundary condition $\psi(x, s(x))$ with $\lambda = 10^{-7}$ in presence of exact boundary data discussed in Example 3.2.

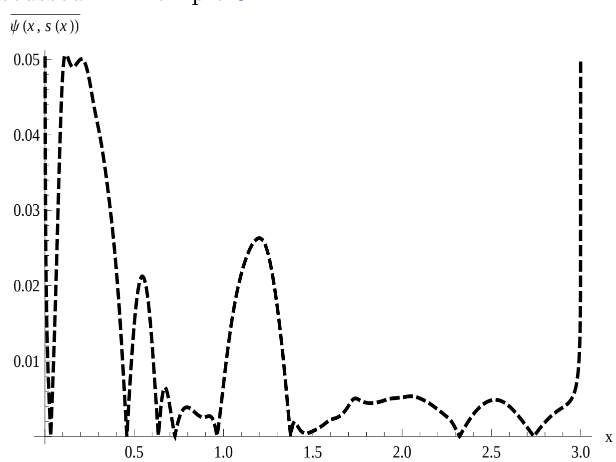

4. CONCLUDING REMARKS

In this article, we approximate the inverse problem of designing the optimal configuration of a conducting body subject to given boundary conditions. As an extra specification, we take advantage of this fact that the volume of the stream function passing through the known region $D \subset \Omega$ gets a desired value. Approximation is based on the combination of the static method of fundamental solutions with the Tikhonov regularization technique to solve the optimization problem. Some numerical examples for various test problems are included to show that the propsed method produces stable solutions with low computational costs.

References

[1] R. Butt, *Optimal shape design for a nozzle problem*, Journal of the Australian Mathematical Society, Ser. B, *35*(1) (1993), 71–86.

[2] J. Cea and E. J. Haug, *Lecture on Optimization Theory and Algorithm*, Cambridge Texts in Applied Mathematics, Springer-Verlag, Berlin, 1978.

[3] M. Dehghan and A. Shokri, *A numerical method for one-dimensional nonlinear Sine-Gordon equation using collocation and radial basis functions*, J. Comput. Appl. Math, *24*(2) (2008), 687–698.

[4] M. H. Farahi, A. H. Borzabadi, H. H. Mehne, and A. V. Kamyad, *Measure theoretical approach for optimal shape design of a nozzle*, J. Appl. Math. Comput, *17*(1-2) (2005), 315–328.

[5] N. Fujii, *Necessary conditions for a domain optimization problem in elliptic boundary value problems*, SIAM J. Control Optim, *24*(3) (1986), 346–360.

[6] M. A. Golberg, C. S. Chen, and Y. F. Rashed, *The annihilator method for computing particular solutions to partial differential equations*, Eng. Anal. Bound. Elem, *23*(3) (1999), 275–279.

[7] M. Hasan, X. W. Tangpong, and O. P. Agrawal, *Fractional optimal control of distributed systems in spherical and cylindrical coordinates*, J. Vib. Control, *18*(10) (2011), 1506–1525.

[8] B. T. Johansson, D. Lesnic, and T. Reeve, *Numerical approximation of the one-dimensional inverse Cauchy-Stefan problem using a method of fundamental solutions*, Invese Probl. Sci. Eng, *19*(5) (2011), 659–677.

[9] A. V. Kamyad and A. H. Borzabadi, *Strong controllability and optimal control of the heat equation with a thermal source*, Korean J. Comput. Appl. Math, *7*(3) (2000), 555–568.

[10] A. V. Kamyad, J. E. Rubio, and D. A. Wilson, *Optimal control of multidimensional diffusion equation*, J. Optim. Theory. Appl, *70*(1) (1991), 191–209.

[11] A. V. Kamyad, J. E. Rubio, and D. A. Wilson, *An Optimal control problem for the multidimensional diffusion equation with a generalized control variable*, J. Optim. Theory. Appl, *75*(1) (1992), 101–132.

[12] A. Karageorghis, D. Lesnic, and L. Marin, *A survey of applications of the MFS to inverse problems*, Inverse Probl. Sci. Eng, *19*(3) (2011), 309–336.

[13] E. Kita and N. Kamiyia, *Trefftz method: An overview*, Adv. Eng. Softw, *24*(1-3) (1995), 3–12.

[14] M. Lakestani and M. Dehghan, *A new technique for solution of a parabolic inverse problem*, Kybernetes, *37*(2) (2008), 352–364.

[15] M. Lakestani and M. Dehghan, *The use of Chebyshev cardinal functions for the solution of a partial differential equation with an unknown time-dependent coefficient subject to an extra measurement*, J. Comput. Appl. Math, *235*(3) (2010), 669–678.

[16] K. Mamehrashi and S. A. Yousefi, *A numerical method for solving a nonlinear 2- D optimal control problem with the classical diffusion equation*, Int. J. Control, *90*(2) (2017), 298–306.

[17] B. Mohammadi and O. Pironneau, *Applied Shape Optimization for Fluids*, Oxford University Press, New York, 2010.

[18] F. Mohebbi and M. Sellier, *Optimal shape design in heat transfer based on body-fitted grid generation*, Int. J. Comput. Methods Eng. Sci. Mech, *14*(3) (2013), 227–243.

[19] F. Mohebbi and M. Sellier, *Three-dimensional optimal shape design in heat transfer based on body-fitted grid generation*, Int. J. Comput. Methods Eng. Sci. Mech, *14*(3) (2013), 473–490.

[20] F. Mohebbi and M. Sellier, *Parameter estimation in heat conduction using a two dimensional inverse analysis*, Int. J. Comput. Methods Eng. Sci. Mech, *17*(4) (2016), 274–287.

[21] F. Murat and J. Simon, *Studies on some optimal shape design problem*, Lecture Notes in Computer Science, Berlin, Springer-Verlag, Berlin, 1976.

[22] A. Myslinski, *Minimax shape optimization problem for von karman systems*, Lecture Notes in Control and Information Sciences, Springer, 2008.

[23] P. W. Partridge and B. Sensale, *The method of fundamental solutions with dual reciprocity for diffusion and diffusion-convection using subdomains*, Eng. Anal. Bound. Elem, *24*(9) (2000), 633–641.

[24] O. Pironneau, *On optimum design in fluid mechanics*, J. Fluid. Mech, *64*(1) (1974), 97–110.

[25] O. Pironneau, *Optimal shape design for elliptic systems*, Springer- Verlag, New York, 1984.

[26] J. A. Rad, K. Rashedi, K. Parand, and H. Adibi, *The meshfree strong form methods for solving one dimensional inverse Cauchy-Stefan problem*, Engineering with Computers, *33*(3) (2017), 547–571.

[27] K. Rashedi, H. Adibi, and M. Dehghan, *Efficient numerical methods for boundary data and righat-hand side reconstructions in elliptic partial differential equations*, Numer. Methods Partial Differ. Equ, *31*(6) (2015), 1995–2026.

[28] K. Rashedi, H. Adibi, and M. Dehghan, *Application of the RitzGalerkin method for recovering the spacewise-coefficients in the wave equation*, Comput. Math. Appl, *65*(12) (2013), 1990–2008.

[29] K. Rashedi, H. Adibi, J. Amani Rad, and K. Parand, *Application of the meshfree methods for solving the inverse one-dimensional Stefan problem*, Eng. Anal. Bound. Elem, *40* (2014), 1–21.

[30] K. Rashedi and A. Sarraf, *Heat source identification of some parabolic equations based on the method of fundamental solutions*, Eur. Phys. J. Plus, (2018), Doi:10.1140/epjp/i2018-12193-8.

[31] T. H. Reeve, *The method of fundamental solutions for some direct and inverse problems*, 2013. Thesis (Ph. D.)–University of Birmingham.

[32] B. Rousselet, *Shape design sensitivity of a membrane*, J. Optim. Theory Appl, *40*(4) (1983), 595–623.

[33] S. Sarabadan, K. Rashedi, and H. Adibi, *Boundary determination of the inverse heat conduction problem in one and two dimensions via the collocation method based on the satisfier functions*, Iran J Sci Technol Trans Sci, *42*(2) (2018), 827–840.

[34] J. Stoer and R. Bulirsch, *Introduction to Numerical Analysis*, Springer-Verlag, New York, 1980.

[35] E. Trefftz, Ein Gegenstuck zum Ritzschen Verfahren, 2^{er} Intern. Kongr. fur Techn. Mech. Zurich, (1926), 131–137.